The gallium isotopic composition of the bulk silicate Earth

Chizu Kato, Frédéric Moynier, Julien Foriel, Fang-Zhen Teng, Igor Puchtel

Chemical Geology 448 (2017) 164–172

Contents lists available at ScienceDirect

Chemical Geology

journal homepage: www.elsevier.com/locate/chemgeo

The gallium isotopic composition of the bulk silicate Earth

Chizu Kato [a,*], Frédéric Moynier [a,b], Julien Foriel [c], Fang-Zhen Teng [d], Igor S. Puchtel [e]

[a] Institut de Physique du Globe de Paris, Université Sorbonne Paris Cité, Université Paris Diderot, 1 rue Jussieu, 75238 Paris cedex 05, France
[b] Institut Universitaire de France, 75005 Paris, France
[c] Earth Life Science Institute, Tokyo Institute of Technology, 2-12-1-IE-1 Ookayama, Meguro, Tokyo 152-8551, Japan
[d] Isotope Laboratory, Department of Earth and Space Sciences, University of Washington, Seattle, WA 98195, USA
[e] Isotope Geochemistry Laboratory, Department of Geology, University of Maryland, College Park, MD 20742, USA

ARTICLE INFO

Article history:
Received 24 July 2016
Received in revised form 10 November 2016
Accepted 16 November 2016
Available online 17 November 2016

Keywords:
Gallium
Bulk Silicate Earth
Basalt
OIB
MORB
Komatiite
MC-ICP-MS

ABSTRACT

We report a new method for precise analysis of gallium (Ga) isotopic composition in geological samples. The purification of Ga is achieved by a three-step ion exchange chromatography to remove matrix and interfering elements. The $^{71}Ga/^{69}Ga$ ratios are analyzed by multi-collector inductively-coupled-plasma mass-spectrometer (MC-ICP-MS). The external reproducibility of the measurements (0.05‰, 2 s.d.) was assessed by replicate analyses of the USGS BCR-2 and BHVO-2 standards. This newly developed technique was then used to investigate the extent of Ga isotopic fractionation during igneous processes by analyzing well-characterized samples from the Kilauea Iki lava lake, USA. These samples were formed in a closed system and have MgO contents ranging from 26.9 to 2.4 wt.%. We found that igneous processes do not fractionate Ga isotopes within the analytical uncertainty and that the Ga isotopic composition of mafic-ultramafic lavas can be used to estimate the composition of their mantle source. Twelve ocean island basalts, two mid-ocean-ridge basalts, one continental flood basalt and one komatiite have homogeneous and nearly identical Ga isotopic compositions within analytical uncertainties averaging 0.00 ± 0.06‰ (2 s.d.). This value represents the best estimate for the Ga isotopic composition of the bulk silicate Earth

1. Introduction

Gallium is a moderately siderophile and moderately volatile element with two stable isotopes, ^{69}Ga and ^{71}Ga, of natural elemental abundance 60.1079 % and 39.8921 %, respectively (Meija et al., 2016). Gallium is moderately incompatible and behaves similar to Al during magmatic differentiation due to their comparable ionic radii, valence and ionization potential (de Argollo and Schilling, 1978) and therefore is enriched in planetary crusts compared to the mantle. Gallium can also substitute for Fe^{3+} due to the similar valence (+III) and ionic radius (Ga^{3+}: 62 pm, Fe^{3+}: 64 pm) in oxidizing environments, but this is secondary to Al^{3+} substitution. As a moderately siderophile element, it is enriched in iron meteorites (up to 100 ppm; Lovering et al., 1957) compared to chondritic meteorites (5– 10 ppm; Lodders and Fegley, 1998). However, due to its moderate volatility ($T_{1/2}$ = 968 K, Lodders, 2003), Ga concentrations vary by about two orders of magnitude between iron meteorite groups as a function of provenance and thermal history, and this fact has been used as an important parameter in iron meteorite classifications (Lovering et al., 1957; Goldberg et al., 1957; Wasson, 1967; Wai and Wasson, 1977, 1979).

The Ga concentration of the bulk silicate Earth (BSE) has been estimated to be ~4 ppm based on mantle xenoliths (O'Neill and Palme, 1998; Jagoutz et al., 1979; McKay and Mitchell, 1988). Using this concentration, McDonough (2003) noticed that Ga falls on the terrestrial volatility trend, suggesting that despite its siderophile behavior, Ga was not incorporated into the Earth's core. Blanchard et al. (2015) suggested that the light element composition of the Earth's core is a major factor in the metal/silicate partitioning of Ga and that this explains its lithophile behavior in the Earth. However, this conclusion was based on extrapolation of low pressure experiments to high pressure conditions of core formation, an approach that can impose large associated errors (Siebert et al., 2013), and therefore requires further experimental investigation. In addition, as a moderately volatile element, Ga displays a widespread depletion in terrestrial planets and in meteorites. For example, carbonaceous chondrites are progressively depleted in Ga, from the CI (~10 ppm) to the CV (~6 ppm) group meteorites (Lodders and Fegley, 1998). The Earth's mantle is even more depleted in Ga (~4 ppm; O'Neill and Palme, 1998) compared to the carbonaceous chondrites. Therefore, if there is virtually no Ga in the Earth's core, there may be only ~2.7 ppm in the bulk Earth from mass balance

* Corresponding author.
E-mail address: kato@ipgp.fr (C. Kato).

http://dx.doi.org/10.1016/j.chemgeo.2016.11.020

calculations. Furthermore, the Moon appears to be more depleted, as evidenced by Ga concentrations in lunar mare basalts that typically are an order of magnitude lower than their terrestrial counterparts (e.g. Warren, 2003).

The isotopic composition of Ga has the potential to be used as a tracer of different processes (evaporation/condensation, metal/silicate partitioning) responsible for its large elemental abundance variations (several order of magnitude) amongst solar system materials. Previous studies on Ga purification by ion exchange were focused on creating chemical fractionation on the columns for isotopic enrichment (e.g. Machlan and Gramlich, 1988; Dembiński et al., 2006) and only few data exist for meteorite or geological standard samples (De Laeter, 1972; Zhang et al., 2016). In this study, we developed a new method for precise determination of the Ga isotopic compositions of terrestrial and meteoritic samples and then applied this method to estimate the Ga isotopic composition of the Earth's mantle. To evaluate the composition of the Earth's mantle, the effects of igneous differentiation on Ga isotopes was estimated by analyzing Kilauea Iki lava lake samples, and tested for the spatial heterogeneity of the Earth's mantle by measuring mafic rocks from different geo-tectonic settings (OIBs, MORBs, CFB), and temporal variability analyzing an Archean komatiite.

2. Samples and methods

2.1. Samples

We have analyzed two USGS standard reference materials (SRM), Columbia River continental flood basalt (BCR-2) and Hawaiian basalt (BHVO-2), Andlau, Bas-Rhin granite (GA), Senones Vosges granite (GS-N), and ocean island basalts (OIBs) from three different locales: the Atlantic ocean (St. Helena, Tristan da Cunha), Indian ocean (Piton de la Fournaise, Reunion Island), and the Pacific ocean (Kilauea Iki lava lake, Hawaii). Two mid-ocean ridge basalt samples (MORB) from the Atlantic Ocean, and a 2.7 Ga komatiite from the Belingwe greenstone belt in the Rhodesian Craton were also analyzed. Mid-ocean ridge basalt sample ARP 74 10-16 is a blocky glassy olivine basalt collected at 2696 m depth, originating from the southwestern side of Mont de Venus located in the FAMOUS area near the mid-Atlantic rift valley (ARCYANA, 1977; Bougault et al., 1979). Ocean island basalts and MORB are mantle-derived rocks that are isotopically distinct in multiple elements (e.g. Sr, Nd, Re, Os, Pb, O), originating from different parts of the mantle (White and Hofmann, 1982; Hauri and Hart, 1993; Jackson and Dasgupta, 2008; Day et al., 2009). The Kilauea Iki lava lake was formed after the 1959 eruption on the southeast part of the Island of Hawaii, when a single eruption filled a previously existing crater, resulting in the formation of a crust roofed lava chamber (Helz, 1980, 2012). The lava cooled in a closed system, and since the lava has the same composition as the country rock, chemical assimilation is minor. Because differentiation of the Kilauea Iki lava lake produced samples with a large range of MgO contents, they have been widely used to evaluate isotopic fractionation during igneous processes (e.g., Li, Tomascak et al., 1999; Mg, Teng et al., 2007; Fe, Teng et al., 2008; Zn, Chen et al., 2013). For this study, eight drill core samples with a wide range of MgO contents have been selected (from 2.4 to 25.8 wt.%).

Komatiites are formed from high temperature magmas with low viscosity, which ascend rapidly preserving the characteristics of the mantle source (Huppert et al., 1985). Komatiite sample TN19 from the Tony's Flow in the 2.7 Ga Belingwe Greenstone Belt, Zimbabwe, previously analyzed by Puchtel et al. (2009) for major and trace elements and Nd and Os isotopic compositions was analyzed.

2.2. Chemical purification of Ga

All samples were ground to a fine powder with agate mortar and pestle, and the weight of each sample for chemistry was then chosen in order to obtain approximately 1 μg of Ga (5 mg to 100 mg depending on Ga concentration of the sample). The samples were then dissolved in a mixture of concentrated HF and HNO_3 (3:1) in closed Teflon vials and heated at a temperature of 120 °C for 72 h to ensure full digestion. Sample solutions were then dried down at 100 °C, then 6 mL of 6 N HCl was added and samples were heated at 120 °C for 24 h in closed beakers to dissolve the fluoride compounds. After digestion, samples were again dried down at 100 °C, then prepared for chemical separation. A protocol for the separation and purification of Ga which involves 3 steps (Table 1) was established. The first step is based on an anion exchange resin to remove matrix elements where Ga is retrieved along with Fe. The second step is to separate Fe from Ga. The last and final step further purifies the solutions, ultimately removing any remaining barium (Ba).

a) Removal of major elements

After sample digestion, all of the dried samples were dissolved in 1 mL of 6 N HCl and loaded on pre-cleaned and pre-conditioned columns. Twenty mL of anion exchange resin AG MP1 (100–200 mesh) in a Bio-Rad Econo-pac chromatography column (diameter 1.5 cm, length 11.5 cm, reservoir volume 250 mL) was used to remove matrix elements. Due to their similarities, Ga^{3+} and Fe^{3+} ions are not separated with this resin and are collected together. Gallium appeared transparent in the columns but ferric chlorides were visible as a yellow band, which provides a visual aid for precise calibration of the collection volume. A total of 40 mL of 6 N HCl is added to remove most elements except Ga^{3+} and Fe^{3+}. Then 10 mL of 0.4 N HCl is added to remove further matrix, before Ga and Fe are retrieved with 20 mL of 0.4 N HCl. Elution results are shown in Table S1 and Fig. S1 in Supplementary materials.

b) Separation of Fe from Ga

Seven mL of cation exchange resin AG 50w-X12 (200–400 mesh) were loaded on a PTFE Teflon column with a diameter of 7 mm, a length

Table 1
Three-step chemical purification method for Ga.

	Eluent	Volume (mL)	Step
Step 1. Matrix removal	H_2O	250	Cleaning
	0.5 N HNO_3	250	Cleaning
	H_2O	250	Cleaning
	0.5 N HNO_3	250	Cleaning
	H_2O	250	Cleaning
	6 N HCl	20	Conditioning
	6 N HCl	1	Sample loading
	6 N HCl	20	Matrix removal
	6 N HCl	20	Matrix removal
	0.4 N HCl	10	Matrix removal
	0.4 N HCl	20	Collection
Step 2. Fe removal	6 N HCl	12	Cleaning
	3 N HCl	12	Conditioning
	3 N HCl	1	Sample loading
	3 N HCl	8	Matrix removal
	3 N HCl	12	Collection
Step 3. Ba removal	H_2O	4	Cleaning
	0.5 N HNO_3	4	Cleaning
	H_2O	4	Cleaning
	0.5 N HNO_3	4	Cleaning
	H_2O	4	Cleaning
	6 N HCl	2	Conditioning
	6 N HCl	0.5	Sample loading
	6 N HCl	4	Matrix removal
	6 N HCl	4	Matrix removal
	0.4 N HCl	4	Collection
	0.4 N HCl	4	Collection

of 27 cm and a reservoir volume of 12 mL. The dried samples from the first step were re-dissolved in 1 mL of 3 N HCl and loaded onto the columns. Iron was first eluted from the column with 8 mL of 3 N HCl, followed by 12 mL of 3 N HCl to elute and collect Ga, which was later dried. Elution results are shown in Table S2 and Fig. S2. After this step, the Fe/Ga is checked, and this step was repeated several times until the Fe/Ga ratio of the sample becomes <0.5, as opposed to ~4000 in the bulk sample.

c) Separation of Ba from Ga

The third column pass is the final step of the column chromatography protocol. The doubly charged Ba ion $^{138}Ba^{++}$ is an interfering isobar to $^{69}Ga^{+}$ due to the same mass/charge ratio. Because Ba has a low potential of ionization and a large fraction of it is doubly ionized, Ba produces a significant contribution at mass 69 which must be minimized by chemical removal of Ba (and later numerical correction) in order to obtain high precision Ga isotopic measurements. For this final step of the column chromatography protocol, the same elution protocol for the first step was used, but with a much smaller volume, in order to remove the remaining Ba. Samples were dissolved in 0.5 mL of 6 N HCl and then passed through a PTFE Teflon column with a diameter of 2 mm, a length of 3 cm and a reservoir volume of 4 mL. After cleaning and conditioning of the resin, the sample dissolved in 0.5 mL of 6 N HCl was loaded on the column, the Ba was eluted with 8 mL of 6 N HCl. Finally, Ga was collected with 8 mL of 0.4 N HCl. Elution results are shown in Table S3 and Fig. S3, and the chemical procedures are given in Table 1.

The yield of the full chemical purification has been estimated several times over the course of this study and has always been found to be better than 95%. The final analytical blank was 0.02 ng, which is negligible compared to the total of >1 μg of Ga analyzed in each of the samples. Chlorine and P were under the detection limit of the MC-ICP-MS in the final solution minimalizing the possibility of $^{37}Cl^{16}O_2$ or $^{40}Ar^{31}P$ interferences.

2.3. Mass spectrometry

The Ga concentration and isotopic ratio were analyzed on a Thermo Fisher Neptune Plus multi-collector inductively-coupled-plasma mass-spectrometer (MC-ICP-MS) at either Washington University in St. Louis, USA or at the Institut de Physique du Globe de Paris (IPGP), France. Samples were dissolved and diluted in a 0.1 N HNO_3 solution to have the same concentration as the standard (25 ppb), and were introduced into the plasma source through an APEX sample introduction system. The APEX heating and cooling temperatures were 120 °C and 2 °C respectively, and a self-aspirating nebulizer with an average uptake rate of 81 μL/min was attached. A blank solution of 0.1 N HNO_3 was measured in the beginning of each sequence and a blank correction was applied. A jet sampler cone and a H skimmer cone was used. A 25 ppb Ga solution yields an intensity between 7 and 9 V, with this variation caused by the ageing of the cones or resolution slit, or variations in the nebulizer uptake rate. Faraday cups equipped with 10^{11} Ω amplifier were positioned to monitor the masses 68 (^{68}Zn), 68.5 ($^{137}Ba^{++}$), 69 (^{69}Ga and $^{138}Ba^{++}$), and 71 (^{71}Ga) with an integration time of 8 s per cycle. Peak centers were taken after tuning and baselines were measured before each measurement. One analysis contained 25 cycles, and was done in low resolution mode. Samples were bracketed using the standard before and after and no fit was used. A 0.1 N HNO_3 cleaning solution was passed through for 160 s after each measurement. To correct for instrumental mass fractionation, standard-sample bracketing was used, with a Ga ICP/DCP standard solution (Aldrich, catalog number 35623-9), which is named Ga IPGP standard hereafter.

Table 2
Observed intensity on masses 68.5, 69, ^{137}Ba and ^{138}Ba and ratios for a 5 ppb Ba standard on the MC-ICP-MS.

Mass	I68.5	I69	^{137}Ba	^{138}Ba	I69/I68.5	$^{138}Ba/^{137}Ba$	$^{138}Ba/^{137}Ba$ lit.
Intensity (V)	0.036	0.23	0.26	1.65	6.39	6.35	6.38[a]

a = Meija et al., 2016

3. Results

3.1. Correction of interfering Ba

Although Ba removal during step 3 of the Ga purification protocol is near complete, the remaining fraction of Ba as well as possible contamination result in a trace amount of Ba in the sample causing an isobaric interference (Table 2). Ba has 7 stable isotopes, masses ^{130}Ba (0.11%), ^{132}Ba (0.10%), ^{134}Ba (2.42%), ^{135}Ba (6.59%), ^{136}Ba (7.85%), ^{137}Ba (11.23%), and ^{138}Ba (71.70%). From concentration measurements of a 5 ppb Ba ICP standard, double ionization measured as $^{138}Ba^{++}/^{138}Ba^{+}$ (mass 69/138) and $^{137}Ba^{++}/^{137}Ba^{+}$ (mass 68.5/137) occurs at a rate of about 14% (Table 2). The doubly ionized ^{138}Ba has the same mass/charge ratio as ^{69}Ga. Because of this interference, a post analysis calculation is needed to remove the effect from the ^{138}Ba on the intensity of the mass 69. The intensity of the ^{137}Ba was monitored at its half mass 68.5.

$$^{69}Ga_{TRUE} = I69 - {}^{138}Ba^{++} \tag{1}$$

$$\frac{^{69}Ga_{TRUE}}{^{71}Ga} = \frac{I69}{^{71}Ga} - \frac{^{138}Ba^{++}}{^{71}Ga} \tag{2}$$

I69 represents the intensity measured on the mass 69 (Eq. (1) and (2)). The true ^{69}Ga intensity ($^{69}Ga_{TRUE}$) is only available after removal of the $^{138}Ba^{++}$ from the intensity on mass 69. I68.5 represents the doubly ionized ^{137}Ba, at the mass of 68.5, ^{71}Ga is the intensity from the sample on mass 71.

$$\frac{^{138}Ba^{++}}{^{71}Ga} = \frac{I68.5}{^{71}Ga} \times \frac{^{138}Ba^{++}}{I68.5} \tag{3}$$

The $^{138}Ba/^{137}Ba$ ratio was 6.35, and I69/I68.5 ratio was 6.39 measured on the MC-ICP-MS, compared to the natural element abundance $^{138}Ba/^{137}Ba = 6.38$. Even though this ratio obtained on the mass spectrometer due to instrumental mass bias is different from the natural ratio, the difference is negligible and does not lead to a significant difference on the corrected $^{71}Ga/^{69}Ga$. Therefore, an approximation can be made, $^{138}Ba^{+}/^{137}Ba^{+} \approx {}^{138}Ba^{++}/^{137}Ba^{++} \approx {}^{138}Ba^{++}/I68.5$ (Eq. (3)). Finally, the data are reported with the conventional delta notation obtained by Eq. (4). The Ba correction was not applied to samples with a negative I68.5 value (Table S4).

$$\delta^{71}Ga = \left[\frac{\left(^{71}Ga/^{69}Ga\right)_{sample}}{\left(^{71}Ga/^{69}Ga\right)_{Ga\ \ IPGP\ \ standard}} - 1 \right] \times 1000 \tag{4}$$

3.2. Verification of post analytical Ba interference correction validity and Ce interference

In order to verify the efficacy of the Ba interference correction method, a 25 ppb Ga IPGP standard doped with a Ba standard with concentrations ranging from 0.5 ppt to 0.5 ppb was measured (Table 3; Fig. 1a). From a Ba/Ga ratio of 4×10^{-4}, the discrepancy between the standard normalized data and Ba interference corrected data became apparent. As the Ba/Ga ratio increased, the sample became isotopically light due to the increase in the mass 69 signal from contribution by the doubly ionized ^{138}Ba. However, accounting for the Ba interference using the

Table 3
Barium interference correction test and Ce interference test.

Ba/Ga (ppb/ppb)	δ^{71}Ga (‰)	Without Ba correction δ^{71}Ga (‰)	Ce/Ga (ppb/ppb)	Without Ce correction δ^{71}Ga (‰)
2.0E-05	0.05	-0.14	2.0E-05	0.00
4.0E-05	n/d	n/d	4.0E-05	0.04
2.0E-04	-0.03	-0.38	2.0E-04	-0.02
4.0E-04	0.00	-0.16	4.0E-04	0.03
1.0E-03	n/d	n/d	1.0E-03	0.00
2.0E-03	0.05	-0.43	2.0E-03	-0.05
3.0E-03	-0.04	-0.75	3.0E-03	0.07
4.0E-03	0.05	-0.72	4.0E-03	0.06
7.5E-03	0.00	-1.58	7.5E-03	n/d
1.0E-02	-0.05	-2.11	1.0E-02	0.17
2.0E-02	-0.03	-4.02	2.0E-02	0.30
4.0E-02	n/d	n/d	4.0E-02	0.39
2.0E-01	n/d	n/d	2.0E-01	2.54
4.0E-01	n/d	n/d	4.0E-01	4.71

68.5 mass effectively corrects this artifact at least up to a Ba/Ga ratio of 2×10^{-2}. A typical pre-chemistry Ba/Ga ratio (Ba/Ga ~ 1000), is always reduced to below Ba/Ga $= 5.0 \times 10^{-4}$ after chemical purification for all the samples presented here validating the efficacy of this method to correct for double charged Ba interference on ^{69}Ga.

The doubly ionized $^{142}Ce^{++}$ ion is an isobar for ^{71}Ga. Although Ce is not as enriched as Ba in terrestrial samples (Ba/Ce ~ 12), it is still concentrated twice as much as Ga. A 25 ppb Ga IPGP standard was doped with Ce concentration of 0.5 ppt to 10 ppb, and its isotopic composition was measured. With increasing Ce/Ga, ratio, the δ^{71}Ga became isotopically heavier (Table 3, Fig. 1b). Since Ce is effectively removed by the first step of the chemistry (Table S1, Fig. S1), and Ce is under the detection limit of the MC-ICP-MS in the final product, this effect was ignored.

3.3. Evaluation test of the reproducibility and accuracy

To confirm that the plasma load did not alter the plasma condition, different concentrations with 10, 30, and 40 ppb Ga IPGP standard were bracketed against a 25 ppb solution. There were no significant isotopic fractionations due to the difference in concentrations (Table 4; Fig. 2). 10 ppb vs 25 ppb had an average value of $\delta^{71}Ga = -0.01 \pm 0.06$‰, 30 ppb vs 25 ppb: $\delta^{71}Ga = 0.00 \pm 0.06$‰, 40 ppb vs 25 ppb: $\delta^{71}Ga = -0.01 \pm 0.06$‰. This confirms that the sample load difference in this range does not affect the isotopic composition. Furthermore, uncertainties in concentration of samples diluted to create a 25 ppb solution are well below the difference tested here.

Several tests were carried out to assess the reproducibility of the chemical chromatography and mass spectrometry. Results are shown in Table 5 and Fig. 3. As a test of precision, a single BHVO-2 sample (BHVO-2 B) was divided into six aliquots, processed through different columns from the second step and measured on the mass spectrometer. BHVO-2 E and BCR-2 were divided in to two aliquots and measured. To further test the reproducibility, the same solutions were measured several times during different analytical sessions. The Ga isotopic compositions of BHVO-2 D, E and F were measured during different analytical sessions (3, 2 and 2, respectively) several months apart (see Table 5). All measurements agreed within 0.05‰.

The absence of isotopic fractionation induced by the chemical purification has been tested by processing BHVO-2 D several times through the column chemistry. After analysis of the sample BHVO-2 D ($\delta^{71}Ga = -0.01 \pm 0.05$‰), which was passed through the second step of column chemistry three times, the leftover solution was processed again through the second step for the fourth time, and 50% of the solution was analyzed ($\delta^{71}Ga = 0.01 \pm 0.14$‰), and 50% of the solution was processed for the fifth time ($\delta^{71}Ga = -0.01 \pm 0.05$‰) (see Table 6). These three replicates of BHVO-2 processed 3, 4 and 5 times through the most delicate part of the chemical purification (second step) are isotopically indistinguishable from each other at the level of the precision and this therefore suggests that the chemical purification during the second step of the chemistry does not fractionate the Ga isotopes. Finally, to test for the possibility of incomplete dissolution or isotopic heterogeneity of the sample, a total procedural replicate (dissolution, chemical purification and mass-spectrometry) of BHVO-2 was prepared (BHVO-2 A to F). When these six independent analyses are taken together we obtain an external reproducibility of 0.05‰ for δ^{71}Ga.

Finally, to further confirm that there was no isotopic fractionation created by the column chemistry, the Ga IPGP standard mixed with major (Al, Fe, Ca) and interfering elements (Ba, Ce) in similar proportions as in BHVO-2 was passed through the chemistry. An aliquot containing 110 ng Ga IPGP standard with 350 μg of Al, 430 μg of Fe, 400 μg of Ca, 190 ng of Ce and 650 ng of Ba from elemental standards were mixed together to create an artificial BHVO-2. This artificial

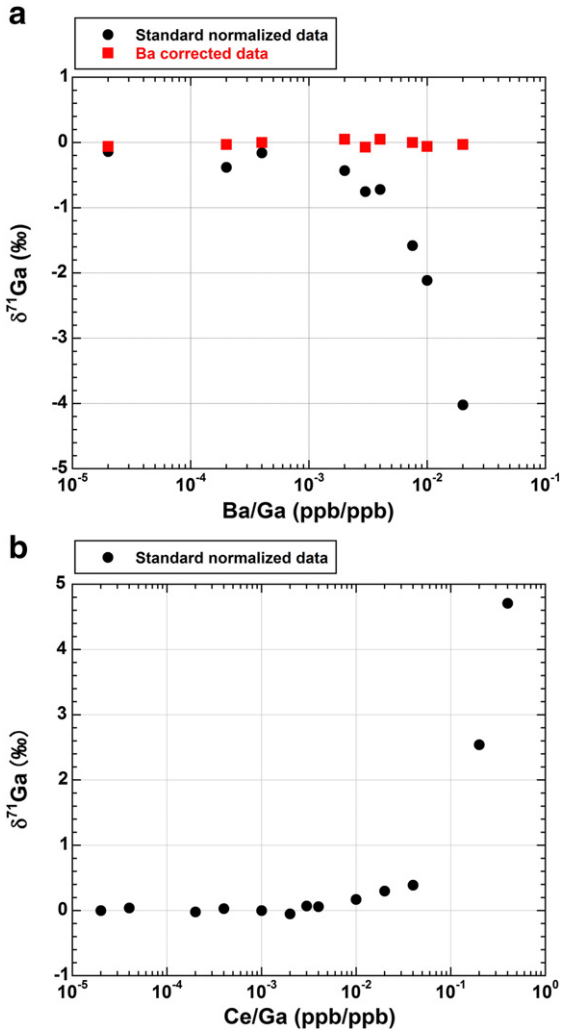

Fig. 1. Doubly charged interference test of Ba and Ce. Black circles represent the δ^{71}Ga obtained from the standard normalized data values, uncertainties are smaller than the symbols. a) δ^{71}Ga versus Ba/Ga ratio for a 25 ppb Ga IPGP standard doped with a Ba standard with various concentrations. Red squares represent the δ^{71}Ga obtained after correction of the Ba interference (see text for details). The data without correction diverts from the $\delta^{71}Ga = 0$‰ and becomes isotopically light after a Ba/Ga ratio of 10^{-3}, whereas the data with the Ba correction is in agreement with the standard up to the maximum Ba/Ga ratio used here (2×10^{-2}). b) δ^{71}Ga versus Ce/Ga ratio for a 25 ppb Ga IPGP standard doped with various Ce standard concentrations. The δ^{71}Ga value becomes isotopically heaver with increasing Ce, with the diversion beginning from 3.0×10^{-3}.

Table 4
Gallium isotopic fractionation test bracketed with different Ga IPGP standard concentrations.

Concentration	δ^{71}Ga (‰)	2 s.d.
10 ppb Ga IPGP std.	0.01	
	0.00	
	−0.05	
10 ppb Ga IPGP std. ave.	**−0.01**	**0.06**
30 ppb Ga IPGP std.	−0.02	
	0.05	
	−0.02	
	0.01	
	0.00	
30 ppb Ga IPGP std. ave.	**0.00**	**0.06**
40 ppb Ga IPGP std.	−0.07	
	−0.02	
	−0.01	
	−0.02	
	0.00	
	0.00	
	−0.03	
	0.00	
	0.04	
	−0.02	
	0.02	
40 ppb Ga IPGP std. ave.	**−0.01**	**0.06**

BHVO-2 had no significant Ga isotopic fractionation compared to the original Ga IPGP standard, with an isotopic value of δ^{71}Ga = −0.01 ± 0.04‰, with a Ga recovery rate of 96% (Table 5).

3.4. Natural samples

Gallium concentrations and isotopic compositions in the samples are reported in Table 7 and Fig. 4a, b and c. The Ga isotopic compositions are reported as per mil deviations from the Ga IPGP standard. A NIST SRM 3119a Gallium (lot 890,709), measured along with the samples during each analytical session, had a relative difference of δ^{71}Ga = 1.38 ± 0.06‰ (2 s.d., n = 15) with the Ga IPGP standard. Due to the large isotopic fractionation between the NIST standard and that of the natural samples, we chose to use the more representative isotopic composition for BSE of the Ga IPGP standard as the reference to report the data.

Although the Ga concentrations in terrestrial samples vary from 2 to 29 ppm, all measured isotopic compositions are within analytical uncertainty of each other ranging from δ^{71}Ga = −0.05 to 0.05‰ with an average δ^{71}Ga = 0.00 ± 0.06‰ (2 s.d., n = 16). In addition, there is no correlation between the elemental concentrations at the level of the analytical precision. The komatiite, which is the sample with the lowest Ga concentration (2.2 ppm), is also isotopically similar to other terrestrial samples with an isotopic composition of 0.02 ± 0.05‰ (2 s.e., n = 9). Kilauea Iki lava lake samples display variation in Ga concentrations, ranging from 11 to 29 ppm, but there are no significant differences in the Ga isotopic composition. Granites GA and GS-N were only measured once, and had an isotopic composition of 0.02‰ and 0.03‰ respectively.

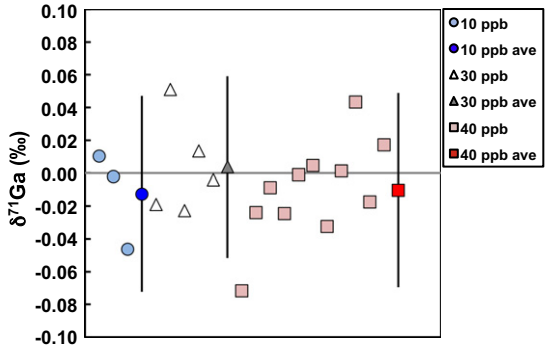

Fig. 2. Gallium isotopic fractionation test with different Ga IPGP standard concentrations. A 10 ppb, 30 ppb and 40 ppb solution were bracketed with a 25 ppb solution. Average values of each concentration are also shown.

Table 5
Gallium isotopic composition and averages for BHVO-2, BCR-2 and artificial BHVO-2.

Sample names	Sample types	δ^{71}Ga (‰)	2 s.d.	n	Ga (ppm)	MgO (wt%)
BHVO-2 B col. 1		0.00		1		
BHVO-2 B col. 2		-0.05		1		
BHVO-2 B col. 3		-0.02		1		
BHVO-2 B col. 4		-0.02		1		
BHVO-2 B col. 5		-0.03		1		
BHVO-2 B col. 6		-0.10		1		
BHVO-2 B ave.	**OIB**	**-0.03**	**0.07**	**6**	**21.7[a]**	**7.23[a]**
BHVO-2 E col. 1		0.03				
		0.00				
BHVO-2 E col. 1 ave.		0.02	0.05	2	21.7[a]	7.23[a]
BHVO-2 E col. 2		-0.04				
		0.05				
		0.07				
BHVO-2 E col 2 ave.		0.03	0.11	3	21.7[a]	7.23[a]
BHVO-2 E ave.	**OIB**	**0.02**	**0.02**	**2**	**21.7[a]**	**7.23[a]**
BHVO-2 D 06/04/2016		-0.02		1	21.7[a]	7.23[a]
BHVO-2 D 13/05/2016		-0.09				
		-0.05				
		-0.02				
		-0.01				
BHVO-2 D 13/05/2016 ave.		-0.04	0.08	4	21.7[a]	7.23[a]
BHVO-2 D 10/06/2016		0.00				
		-0.02				
BHVO-2 D 10/06/2016 ave..		-0.01	0.03	2	21.7[a]	7.23[a]
BHVO-2 D 30/08/2016		0.02				
BHVO-2 D ave.	**OIB**	**-0.01**	**0.05**	**4**	**21.7[a]**	**7.23[a]**
BHVO-2 F 06/04/2016		-0.02		1	21.7[a]	7.23[a]
BHVO-2 F 10/06/2016		0.00				
		-0.04				
BHVO-2 F 10/06/2016 ave.		-0.02	0.06	2	21.7[a]	7.23[a]
BHVO-2 F 30/08/2016		0.04			21.7[a]	7.23[a]
BHVO-2 F ave.	**OIB**	**0.00**	**0.06**	**3**	**21.7[a]**	**7.23[a]**
BHVO-2 A		0.01				
		0.00				
BHVO-2 A ave.	**OIB**	**0.00**	**0.01**	**2**	**21.7[a]**	**7.23[a]**
BHVO-2 C	**OIB**	**-0.05**		**1**	**21.7[a]**	**7.23[a]**
BHVO-2 A, B, C, D, E, F ave.		**-0.01**	**0.05**	**6**	**21.7[a]**	**7.23[a]**
BCR-2 col. 1		-0.01		1	23[b]	3.59[b]
BCR-2 col. 2		0.00				
		-0.02				
		-0.01				
BCR-2 col. 2 ave.		-0.01	0.03	3	23[b]	3.59[b]
BCR-2 ave.	**CFB**	**-0.01**	**0.01**	**2**	**23[b]**	**3.59[b]**
Artificial BHVO-2		-0.03				
		0.00				
Artificial BHVO-2 ave.		**-0.01**	**0.04**	**2**	**Ga recovery rate 96 %**	

a = Wilson 1997a, b = Wilson 1997b.

4. Discussion

4.1. Reproducibility and accuracy of the method

A BHVO-2 and BCR-2 were measured for the full reproducibility of the chemical and instrumental procedure. Total procedural replicates (i.e. dissolution, chemical purification and mass-spectrometry) of BHVO-2 (BHVO-2 A, B, C, D, E and F) were tested and all six BHVO-2 samples agree within each replicate uncertainty. The obtained average value of the six replicates is −0.01 ± 0.05‰ (2 s.d. n = 6). We therefore use this error as the external reproducibility. In addition, the average for a single BCR-2 divided into two aliquots is δ^{71}Ga = −0.01 ± 0.01‰ (2 s.d., n = 2). Similar reproducibility to BHVO-2 and BCR-2 was obtained on other samples (see Table 7). Two replicates of the St. Helena's basalt SH25 are in good agreement with an average value of δ^{71}Ga = 0.01 ± 0.02‰ (2 s.d.). KI 67-2-85.7 exhibit an average value of δ^{71}Ga = 0.01 ± 0.05‰ (2 s.d., n = 7), which is confirmed by the full

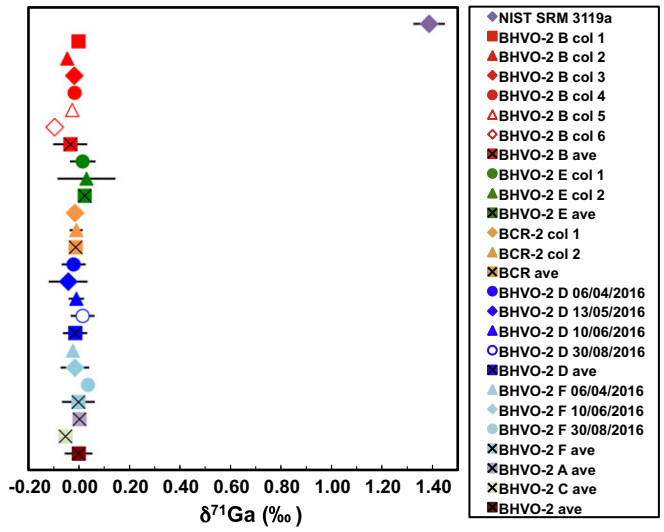

Fig. 3. Test results of the reproducibility of the chemical purification and isotopic measurement of Ga, represented as δ^{71}Ga normalized to the Ga IPGP standard. Each full procedure replicate measured during different MC-ICP-MS sessions of BHVO-2 give a homogeneous isotopic composition with an external reproducibility of 0.05‰ (2 s.d.). NIST SRM 3119a Ga standard has a value of δ^{71}Ga = 1.38 ± 0.06‰ (2 s.d.).

procedural replicates (n = 4) with a value of δ^{71}Ga = −0.01 ± 0.07‰ (2 s.d.). The derived average value for KI 67-2-85.7 is δ^{71}Ga = 0.00 ± 0.03‰ (2 s.d.). KI 67-3-58.0 also agrees with its full procedural replicate within error, with values of δ^{71}Ga = 0.00 ± 0.06‰ (2 s.d.) and δ^{71}Ga = 0.04 ± 0.03‰ (2 s.d.). Finally, no isotopic variations were observed (no more than 0.06‰) for sample solutions analyzed months apart in different sessions for BHVO-2 D, E and F, implying a lack of any seasonal variation in the data. Therefore, all these tests support the robustness of the method and demonstrate satisfying reproducibility.

The BHVO-2 tests that were carried out do not completely rule out a systematic isotopic fractionation on the columns since the true value of BHVO-2 or BCR-2 is unknown. In order to address this, an artificial BHVO-2 that was created from the Ga IPGP standard and other major and interfering elements, and its isotopic composition agree within error with the non-matrix induced Ga IPGP standard after chemistry and applying the Ba correction. Furthermore, a similar relative difference between BHVO-2 and BCR-2 with Zhang et al. (2016) was obtained (Zhang et al., 2016 = 0.02 ± 0.03‰, this study = 0.00 ± 0.05‰).

4.2. Absence of Ga isotopic fractionation during fractional crystallization in a closed system

The original 1959 Kilauea Iki lava is a picrite with the emplaced lava having an average MgO content of 15.4 wt.% (Wright, 1973). The chemical compositions of these fast cooling eruption samples are controlled mainly by variations in the olivine content. Core samples from Kilauea

Table 6
Chemical reproducibility test for the second step of Ga purification method using a BHVO-2 sample.*

Procedure	δ^{71}Ga (‰)	2 s.d.	2 s.e.	n
BHVO-2 D (3) ave	**−0.01**	**0.05**	**0.02**	**4**
Fourth pass chemistry				
BHVO-2 D (4)	−0.04			
	0.06			
BHVO-2 D (4) ave	**0.01**	**0.14**	**0.10**	**2**
Fifth pass chemistry				
BHVO-2 D (5)	−0.01			
BHVO-2 D (5) ave	**−0.01**	**0.05***		**1**

* Used the external reproducibility for the δ^{71}Ga (‰).

Table 7
Average Ga isotopic composition and Ga concentration of samples measured in this study.

Sample names	Sample types	δ^{71}Ga (‰)	2 s.d.	n	Ga (ppm)	MgO (wt.%)
St. Helena SH25	OIB	0.02				
		0.02				
		0.02				
ave.		0.02	0.00	3	25[a]	13.99[f]
St. Helena SH25 replicate	OIB	−0.01				
		−0.03				
		−0.03				
		−0.01				
		0.01				
		0.00				
		0.04				
		0.05				
ave.		0.00	0.06	8	25[a]	13.99[f]
St. Helena SH25 ave.		**0.01**	**0.02**	**2**	**25[a]**	**13.99[f]**
Tristan da Cunha	OIB	0.05				
		0.05				
		0.03				
Tristan da Cunha ave.		**0.04**	**0.02**	**3**	**22[a]**	**17.83[g]**
Reunion Island	OIB	−0.02				
		−0.04				
		−0.07				
Reunion Island ave.		**−0.04**	**0.05**	**3**	**10[a]**	**20.63[g]**
ARP 74 10-16 DR	MORB	−0.01				
MORB Glass		−0.10				
MORB Glass ave.		**−0.05**	**0.13**	**2**	**13[a]**	**10.66[h]**
ARP 74 10-16 DR	MORB	−0.04				
MORB Core		−0.03				
MORB Core ave.		**−0.03**	**0.00**	**2**	**16[a]**	**10.13[i]**
GA	**Granite**	**0.02**	**0.05***	**1**	**16[b]**	**0.95[b]**
GS-N	**Granite**	**0.03**	**0.05***	**1**	**22[c]**	**2.3[c]**
TN 19	Komatiite	0.13				
		0.01				
		0.02				
		0.00				
		0.07				
		0.11				
		−0.15				
		0.03				
		0.00				
TN 19 ave.		**0.02**	**0.16**	**9**	**2.2[a]**	**30.3[j]**
KI 81-2-88.6	OIB	0.03				
		0.02				
		0.00				
		0.03				
KI 81-2-88.6 ave.		**0.02**	**0.03**	**4**	**29[a]**	**2.37[k]**
KI 79-3-150.4	OIB	0.10				
		0.06				
		0.02				
		0.02				
KI 79-3-150.4 ave.		**0.05**	**0.08**	**4**	**13[a]**	**13.5[k]**
KI 75-1-121.5	OIB	−0.02				
		0.01				
ave.		0.00	0.04	2	17[a]	7.77[k]
KI 75-1-121.5 replicate	OIB	−0.09				
		−0.06				
		−0.05				
		−0.06				
ave.		−0.07	0.04	4	19[a]	7.77[k]
KI 75-1-121.5 ave.		**−0.03**	**0.09**	**2**	**18[a]**	**7.77[k]**
KI 67-2-85.7	OIB	0.06				
		0.01				
		0.02				
		−0.02				
		0.02				
		−0.02				
		0.03				
ave.		0.01	0.05	7	24[a]	2.6[k]
KI 67-2-85.7 replicate	OIB	0.01				
		0.03				
		−0.01				
		−0.06				
ave.		−0.01	0.07	4	26[a]	2.6[k]
KI 67-2-85.7 ave.		**0.00**	**0.03**	**2**	**25[a]**	**2.6[k]**

Table 7 (*continued*)

Sample names	Sample types	δ^{71}Ga (‰)	2 s.d.	n	Ga (ppm)	MgO (wt.%)
KI 67-3-58.0	OIB	0.03				
		0.01				
		0.00				
		−0.04				
ave.		0.00	0.06	4	14[a]	8.91[k]
KI 67-3-58.0 replicate	OIB	0.06				
		0.02				
		0.02				
		0.05				
ave.		0.04	0.03	4	13[a]	8.91[k]
KI 67-3-58.0 ave.		**0.02**	**0.05**	**2**	**13.5[a]**	**8.91[k]**
KI 79-1R1-170.9	OIB	−0.01				
		−0.02				
		0.04				
		0.02				
ave.		0.01	0.06	4	23[a]	3.48[k]
KI 79-1R1-170.9 replicate	OIB	0.05				
		0.05				
		0.03				
		0.08				
ave.		0.05	0.04	4	22[a]	3.48[k]
KI 79-1R1-170.9 ave.		**0.03**	**0.07**	**2**	**22.5[a]**	**3.48[k]**
KI 67-3-6.8	OIB	−0.04				
		−0.05				
ave.		−0.04	0.02	2	11[a]	25.83[k]
KI 67-3-6.8 replicate	OIB	−0.04				
		0.01				
ave.		−0.01	0.07	2	11[a]	25.83[k]
KI 67-3-6.8 ave		**−0.03**	**0.04**	**2**	**11[a]**	**25.83[k]**
KI 75-1-75.2	OIB	0.00				
		0.02				
ave.		0.01	0.03	2	21[a]	5.77[k]
KI 75-1-75.2 replicate	OIB	0.01				
		0.03				
ave.		0.02	0.02	2	22[a]	5.77[k]
KI75-1-75.2 ave		**0.01**	**0.01**	**2**	**21.5[a]**	**5.77[k]**
		Total Ave.	**2 s.d.**	**n**		
Total average (including BHVO-2 and BCR-2)		**0.00**	**0.06**	**16**		
NIST SRM 3119a	**NIST STD**	**1.38**	**0.06**	**15**		

a = This study, b = Govindaraju and Roelandts, 1988, c = Govindaraju and Roelandts, 1989, d = Wilson, 1997a, e = Wilson, 1997b, f = Kawabata et al., 2011, g = Humphreys and Niu, 2009, h = Fujii and Bougault, 1983, i = ARCYANA, 1977, j = Puchtel et al., 2009, k = Heltz, 2012.

* Used the external reproducibility as error for δ^{71}Ga (‰).

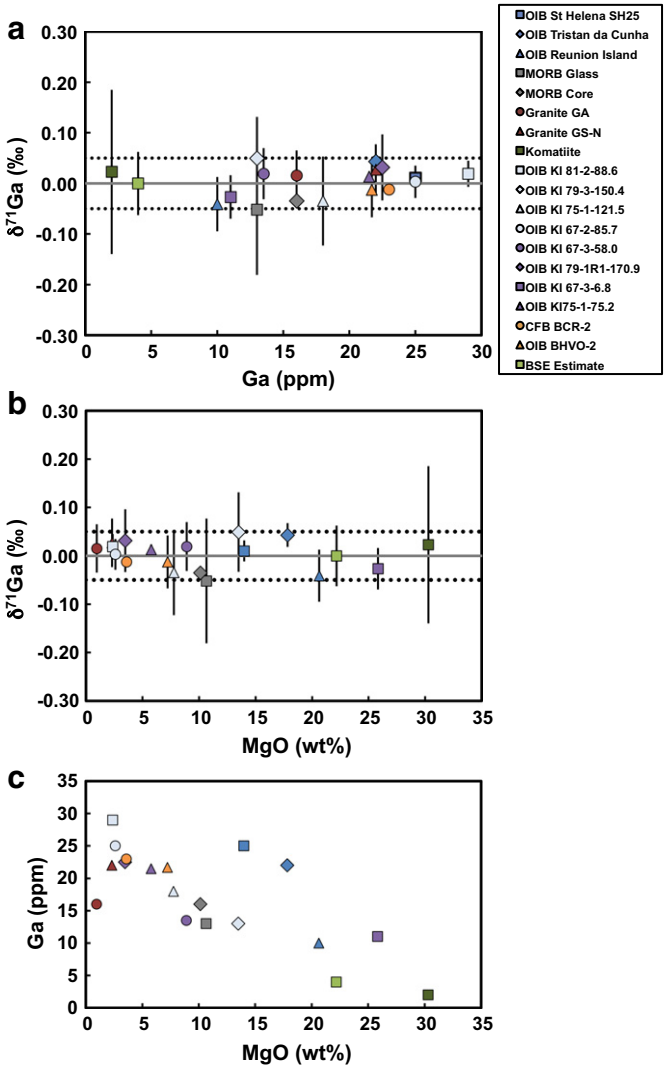

Fig. 4. Results of Ga isotopic compositions, Ga concentrations and MgO concentrations in samples. a) Ga isotopic composition versus Ga concentrations of samples. No significant correlation between the Ga isotopic composition and its concentration is observed. BSE estimate value is shown as the light green square along with the dotted line showing the error with a δ^{71}Ga value of 0.00 ± 0.05‰, and a Ga concentration of 4 ppm (Palme and O'Neill, 2003). b) Ga isotopic composition versus MgO (wt.%) from literature. There is no significant correlation between the Ga isotopic composition and MgO concentration. c) Ga concentration versus MgO (wt.%) from literature. Reverse correlation between the Ga concentration and MgO concentration can be observed.

Iki lava lake range from olivine-rich cumulates, through olivine tholeiites, ferrodiabases and andesites (Helz and Thornber, 1987). The samples utilized in this study include two eruption lavas (Iki-22, Iki-58) and 8 drill core samples from the interior of the lake, and therefore provide a large spectrum of lithologies. These samples have been well characterized in previous studies for major and trace elements, with MgO contents ranging from 25.8 to 2.4 wt.%, and 44.6 to 57.1 wt.% for SiO_2 wt.%, as well as Li, Mg and Fe isotopes (Helz et al., 1994; Tomascak et al., 1999; Teng et al., 2007, 2008, 2011; Pitcher et al., 2009; Helz, 2012).

Kilauea Iki lava lake was formed during a single eruption and internal fractional crystallization has produced a wide range of bulk chemical compositions. The chemical composition of the most MgO rich samples (MgO > 7.5 wt.%) is controlled by the removal or addition of olivine, whereas the most evolved samples (MgO < 7.5 wt.%) are formed by extraction of a liquid from a crystal mush wherein crystallization of augite, Fe-Ti oxides and plagioclases occurred (Helz, 2012). Fractional crystallization and crystal settling has produced samples with different Ga contents, ranging from 11 to 29 ppm and Ga is negatively correlated with the MgO wt.% (Fig. 4c), which is a consequence of the incompatibility of Ga in olivine. This observation is in agreement with a previous study of Hawaiian basalts by Wasson and Baedecker (1970) that observed an increase in Ga concentration in the residual magma. On the other hand, there is no correlation between the Ga isotopic composition and the MgO (or Ga) abundances (Fig. 4a and b).

We can therefore conclude that igneous processes have limited effects on the isotopic composition of Ga (<0.05‰ for δ^{71}Ga), implying that the isotopic compositions of basalts can be used as a proxy for their mantle sources. These results are similar to those observed for Mg (Teng et al., 2007), for which no isotopic fractionation (<0.1‰ for δ^{26}Mg) was observed in the same samples. Additionally, two granites have isotopic compositions that are indistinguishable from mafic and ultramafic rocks (Table 7) at the level of the current precision, further indicating a lack of significant Ga isotopic fractionation during magmatic differentiation.

4.3. Gallium isotopic composition in the bulk silicate Earth

Kilauea Iki lava lake samples show that high temperature igneous processes do not fractionate Ga isotopes at the current level of precision. This implies that mantle-derived mafic and ultramafic rocks can be used

to determine the isotopic composition of the mantle. The Ga isotopic compositions of mafic and ultra-mafic lavas from different tectonic settings (e.g. continental flood basalts such as BCR-2 vs OIB and MORBs), mantle sources (OIBs from different mantle end-members), depths of melting (MORBs vs OIBs), and degrees of partial melting (komatiites vs basalts) all have a homogeneous Ga isotopic composition averaging $\delta^{71}Ga = 0.00 \pm 0.06‰$ (2 s.d.). This indicates that the Ga isotopic composition of the mantle is homogeneous within the analytical uncertainty. The lack of resolvable Ga isotopic fractionation during igneous differentiation suggests that the Ga isotopic composition of planetary crusts and primitive meteorites can be directly compared. The next step is to study the effects of Ga metal-silicate partitioning at relevant pressures and temperatures to evaluate the effect of core formation on the Ga isotopic composition of the bulk Earth. In addition, it has recently been shown that the isotopic composition of moderately volatile elements can be used to study the origin of the volatile depletion of the Moon (e.g. Day and Moynier, 2014; Kato et al., 2015; Wang and Jacobsen, 2016). Since Ga is depleted by a factor 10 between terrestrial and lunar basalts (Warren, 2003), Ga isotopes may hold valuable insights with regards to the volatile depletion of the Moon.

5. Conclusions

We have developed a chemical chromatography procedure to purify Ga from rock samples. The three-step ion-exchange chromatography coupled with MC-ICP-MS isotopic measurements allows to measure the Ga isotopic composition with an external reproducibility of 0.05‰ (2 s.d).

We applied this method to study a series of samples from the Kilauea Iki lava lake and show that igneous differentiation does not fractionate Ga within the analytical uncertainty and that basalts have the same composition as their mantle source. We analyzed the Ga isotopic composition of a variety of terrestrial mafic and ultra-mafic samples and evaluate the $\delta^{71}Ga$ of the BSE to be $0.00 \pm 0.06‰$ (2 s.d., $n = 16$). These observations suggest that the Ga isotopic signature of a given component of a magmatic reservoir that has undergone igneous differentiation can be used as a proxy for the bulk reservoir, e.g. the crustal Ga isotopic signatures of terrestrial, lunar, and Martian crustal material accurately represent the Ga isotopic signature of the bulk mantle of these respective bodies.

Supplementary data to this article can be found online at http://dx.doi.org/10.1016/j.chemgeo.2016.11.020.

Acknowledgements

FM acknowledges funding from the European Research Council under the H2020 framework program/ERC grant agreement #637503 (Pristine), as well as the financial support of the UnivEarthS Labex program at Sorbonne Paris Cité (ANR-10-LABX-0023 and ANR-11-IDEX-0005-02), and the ANR through a chaire d'excellence Sorbonne Paris Cité. We would like to thank Martin Schiller, two anonymous reviewers and journal editor Klaus Mezger for greatly improving the manuscript and pointing out several mistakes in the original submission. For the discussions, we would like to thank Francis Albarède, Paolo Sossi, Bruce Fegley Jr., Katharina Lodders, Ingrid Blanchard and Hugh O'Neill. Finally, special thanks to Brandon Mahan and Nicholas Badullovich for proofreading the manuscript.

References

ARCYANA, 1977. Rocks collected by bathyscaph and diving saucer in the FAMOUS area of the Mid-Atlantic Rift Valley: petrological diversity and structural setting. Deep. Res. 24.

Blanchard, I., Badro, J., Siebert, J., Ryerson, F.J., 2015. Composition of the core from gallium metal–silicate partitioning experiments. Earth Planet. Sci. Lett. 427:191–201. http://dx.doi.org/10.1016/j.epsl.2015.06.063.

Bougault, H., Cambon, P., Corre, O., Joron, J.L., Treuil, M., 1979. Evidence for variability of magmatic processes and upper mantle hetrogeneity in the axial region of the mid-atlantic ridge near 22° and 36 N°. Tectonophysics 55, 11–34.

Chen, H., Savage, P.S., Teng, F.Z., Helz, R.T., Moynier, F., 2013. Zinc isotope fractionation during magmatic differentiation and the isotopic composition of the bulk Earth. Earth Planet. Sci. Lett. 369-370, 34–42.

Day, J.M.D., Moynier, F., 2014. Evaporative fractionation of volatile stable isotopes and their bearing of the origin of the Moon. Philos. Trans. A Math. Phys. Eng. Sci. 372, 20130259.

Day, J.M.D., Pearson, D.G., Macpherson, C.G., Lowry, D., Carracedo, J.C., 2009. Pyroxenite-rich mantle formed by recycled oceanic lithosphere: Oxygen-osmium isotope evidence from Canary Island lavas. Geology 37, 555–558.

de Argollo, R.M., Schilling, J.-G., 1978. Ge/Si and Ga/Al variations along the Reykjanes Ridge and Iceland. Nature 276:24–28. http://dx.doi.org/10.1017/CBO9781107415324.004.

De Laeter, J.R., 1972. The isotopic composition and elemental abundance of gallium in meteorites and in terrestrial samples. Geochim. Cosmochim. Acta 36, 735–743.

Dembiński, W., Herdzik, I., Skwara, W., Bulska, E., Wysocka, A.I., 2006. Isotope Effects of Gallium and Indium in Cation Exchange Chromatography. 51 pp. 1–4.

Fujii, T., Bougault, H., 1983. Melting relations of a magnesian abyssal tholeiite and the origin of MORBs. Earth Planet. Sci. Lett. 62, 283–295.

Goldberg, E., Uchiyama, A., Brown, H., 1957. The distribution of nickel, cobalt, gallium, palladium and gold in iron meteorites. Geochim. Cosmochim. Acta 2, 1–25.

Govindaraju, K., Roelandts, I., 1988. Compilation report (1966–1987) on trace elements in five CRPG geochemical reference samples: basalt BR; granites, GA and GH; micas, biotite mica-Fe and phlogopite mica-Mg. Geostand. Newslett. 12, 119–201.

Govindaraju, K., Roelandts, I., 1989. Compilation of working values and sample description for 272 geostandards. Geostand. Newslett. 13, 1–113.

Hauri, E.H., Hart, S.R., 1993. ReOs isotope systematics of HIMU and EMII oceanic island basalts from the south Pacific Ocean. Earth Planet. Sci. Lett. 114, 353–371.

Helz, R.T., 1980. Crystallization history of Kilauea Iki lava lake as seen in drill core recovered in 1967–1979. Bull. Volcanol. 43, 675–701.

Helz, R.T., 2012. Trace-element analyses of core samples from the 1967–1988 drillings of Kilauea Iki Lava Lake, Hawaii. US Geological Survey Open File Report 2012–1050, pp. 1–56.

Helz, R.T., Thornber, C.R., 1987. Geothermometry of Kilauea Iki lava lake, Hawaii. Bull. Volcanol. 49, 651–668.

Helz, R.T., Kirschenbaum, H., Marieneko, J.W., Qian, R., 1994. Whole-rock analyses of core samples from the 1967, 1975, 1979 and 1981 drillings of Kilauea Iki lava lake, Hawaii. US Geological Survey Open File Report 94–684, pp. 1–65.

Humphreys, E.R., Niu, Y., 2009. On the composition of ocean island basalts (OIB): The effects of lithospheric thickness variation and mantle metasomatism. Lithos 112, 118–136.

Huppert, H.E., Stephen, R., Sparks, J., 1985. Cooling and contamination of mafic and ultramafic magmas during ascent through continental crust. Earth Planet. Sci. Lett. 74, 371–386.

Jackson, M.G., Dasgupta, R., 2008. Compositions of HIMU, EM1, and EM2 from global trends between radiogenic isotopes and major elements in ocean island basalts. Earth Planet. Sci. Lett. 276, 175–186.

Jagoutz, E., Palme, H., Baddenhausen, H., Blum, K., Cendales, M., Dreibus, G., Spettel, B., Lorenz, V., Wänke, H., 1979. The abundances of major, minor and trace elements in the earth's mantle as derived from primitive ultramafic nodules. Proc. 10th Lunar Planet. Sci. Conf, pp. 2031–2050.

Kato, C., Moynier, F., Valdes, M.C., Dhaliwal, J.K., Day, J.M.D., 2015. Extensive volatile loss during formation and differentiation of the Moon. Nat. Commun. 6:7617. http://dx.doi.org/10.1038/ncomms8617.

Kawabata, H., Hanyu, T., Chang, Q., Kimura, J.-I., Nichols, A.R.L., Tatsumi, Y., 2011. The petrology and geochemistry of St. Helena alkali basalts: Evaluation of the oceanic crust-recycling model for HIMU OIB. J. Petrol. 52, 791–838.

Lodders, K., 2003. Solar system abundances and condensation temperatures of the elements. Astrophys. J. 591, 1220–1247.

Lodders, K., Fegley, B.J., 1998. The Planetary Scientist's Companion. Oxford University Press.

Lovering, J., Nichiporuk, W., Chodos, A., Brown, H., 1957. The distribution of gallium, germanium, cobalt, chromium, and copper in iron and stony-iron meteoritea in relation to nickel content and structure. Geochim. Cosmochim. Acta 11, 263–278.

Machlan, L.A., Gramlich, J.W., 1988. Isotopic fractionation of gallium on an ion-exchange column. Anal. Chem. 60, 37–39.

McDonough, W.F., 2003. Compositional model for the Earth's core. In: Carlson, R.W. (Ed.), Treatise on Geochemistry, The Mantle and Core vol. 2. Elsevier Press, New York, pp. 547–568.

McKay, D.B., Mitchell, R.H., 1988. Abundance and distribution of gallium in some spinel and garnet lherzolites. Geochim. Cosmochim. Acta 52, 2867–2870.

Meija, J., Coplen, T.B., Berglund, M., Brand, W.A., De Bièvre, P., Gröning, M., Holden, N.E., Irrgeher, J., Loss, R.D., Walczyk, T., Prohaska, T., 2016. Isotopic compositions of the elements 2013 (IUPAC technical report). Pure Appl. Chem. 88, 293–306.

O'Neill, H.S.C., Palme, H., 1998. Composition of the silicate Earth: implications for accretion and core formation. In: Jackson, I. (Ed.), The Earth's Mantle: Composition, Structure, and Evolution. Cambridge University Press, Cambridge, pp. 3–126.

Palme, H., O'Neill, H.S.C., 2003. Cosmochemical estimates of mantle composition. In: Carlson, R.W. (Ed.), Treatise on Geochemistry, The Mantle and Core vol. 2. Elsevier Press, New York, pp. 1–38.

Pitcher, L., Helz, R.T., Walker, R.J., Piccoli, P., 2009. Fractionation of the platinum-group elments and Re during crystallization of basalt in Kilauea Iki lava Lake, Hawaii. Chem. Geol. 260, 196–210.

Puchtel, I.S., Walker, R.J., Brandon, A.D., Nisbet, E.G., 2009. Pt-Re-Os and Sm-Nd isotope and HSE and REE systematics of the 2.7 Ga Belingwe and Abitibi komatiites. Geochim. Cosmochim. Acta 73, 6367–6389.
Siebert, J., Badro, J., Antonangeli, D., Ryerson, F.J., 2013. Terrestrial accretion under oxidizing conditions. Science 339, 1194–1197.
Teng, F.Z., Wadhwa, M., Helz, R.T., 2007. Investigation of magnesium isotope fractionation during basalt differentiation: Implications for a chondritic composition of the terrestrial mantle. Earth Planet. Sci. Lett. 261, 84–92.
Teng, F.-Z., Dauphas, N., Helz, R.T., 2008. Iron isotope fractionation during magmatic differentiation in Kilauea Iki lava lake. Science 320, 1620–1622.
Teng, F.Z., Dauphas, N., Helz, R.T., Gao, S., Huang, S., 2011. Diffusion-driven magnesium and iron isotope fractionation in Hawaiian olivine. Earth Planet. Sci. Lett. 308, 317–324.
Tomascak, P.B., Tera, F., Helz, R.T., Walker, R.J., 1999. The absence of lithium isotope fractionation during basalt differentiation: new measurements by multicollector sector ICP-MS. Geochim. Cosmochim. Acta 63, 907–910.
Wai, C.M., Wasson, J.T., 1977. Nebular condensation of moderately volatile elements and their abundances in ordinary chondrites. Earth Planet. Sci. Lett. 36, 1–13.
Wai, C.M., Wasson, J.T., 1979. Nebular condensation of Ga, Ge and Sb and the chemical classification of iron meteorites. Nature 282, 790–793.
Wang, K., Jacobsen, S.B., 2016. Potassium isotopic evidence for the origin of the moon. Submitt. to Nat.:1–10, http://dx.doi.org/10.1038/nature19341.
Warren, P.H., 2003. The moon. In: Davis, A.M. (Ed.), Meteorites, Comets, and Planets Vol. 1. Elsevier-Pergamon, Amsterdam, pp. 559–599.
Wasson, J.T., 1967. The chemical classification of iron meteorites: I. A study of iron meteorites with low concentrations of gallium and germanium. Geochim. Cosmochim. Acta 31, 161–180.
Wasson, J.T., Baedecker, P.A., 1970. Ga, Ge, In, Ir and Au in lunar, terrestrial and meteoritic basalts. Proc. Apollo 11 Lunar Sci. Conf. 2, pp. 1741–1750.
White, W.M., Hofmann, A.W., 1982. Sr and Nd isotope geochemistry of oceanic basalts and mantle evolution. Nature 296, 821–825.
Wilson, S.A., 1997a. Data compilation for USGS reference material BHVO-2. Hawaiian Basalt. U.S. Geological Survey Open-File Report.
Wilson, S.A., 1997b. The collection, preparation and testing for USGS reference material BCR-2, Columbia River. Basalt U.S. Geological Survey Open-File Report.
Wright, T.L., 1973. Magma mixing as illustrated by the 1959 eruption, Kilauea volcano, Hawaii. Geol. Soc. Am. Bull. 84, 849–858.
Zhang, T., Zhou, L., Yang, L., Wang, Q., Feng, L., Liu, Y., 2016. High precision measurements of gallium isotopic compositions in geological materials by MC-ICP-MS. J. Anal. At. Spectrom. 0, 1–7.